IMPROVING SEGMENTATION MAPS USING POLARIZATION IMAGING

Jawad Elsayed Ahmad, Yoshitate Takakura

Université Louis Pasteur, Strasbourg I
Laboratoire des Sciences de l'Image et de la Télédétection UMR 7005 CNRS,
Boulevard Sébastien Brant, 67412 Illkirch, France
E-mail: jawadsayed@termxjy.u-strasbg.fr ; yt@mephot.u-strasbg.fr

ABSTRACT

Within the frame of polarimetric imagery, segmentation of 4×4 Mueller images consists in isolating objects that have different polarizing properties. Such objects are either partial polarizers, rotators or phasors. This means that there are 3 main polarization classes to consider. The difficulty in polarimetric segmentation comes from the fact that the relations between each of the mentioned class and the 4×4 elements of a Mueller matrix are not completely identified. Rather than dealing with unidentified quantities, Mueller images are transformed into intensity images so that robust classical segmentation procedures such as Hidden Markov Chain (HMC) can be applied. Such transformation is possible because it is the reversion procedure of the Mueller matrices retrieval procedure. Also, it is worth mentioning that the noise in the intensity images can be inferred so that the approach is mathematically rigorous. When applied to simulated or recorded images, it appears that the method outperforms approaches based on direct segmentation of Mueller images.

Index Terms— Polarimetry, Clustering methods, Hidden Markov models

1. INTRODUCTION

Clustering algorithms play a major role in simplifying the interpretation and understanding of observed scenes. The robustness of any clustering technique heavily depends on the enclosed information within the image acquired by the imaging system. Classically most of the conventional imaging systems are based on the following principle: a scene is illuminated by light, an optical lens collect the scene radiance and maps it on a CCD camera. After that, a dedicated segmentation algorithm will be implemented in order to cluster different regions having the same intensity reflectivity. In some particular cases the presence of highly reflective objects may cause a blindness of the camera, also in the presence of transparent objects, segmentation methods reposing on a conventional intensity image seem to be powerless.

In contrast, by controlling the polarization state of light we can overcome such problems. Thus a more precise segmentation map could be extracted using the same segmentation algorithm by simply replacing conventional intensity images by polarization one. In this paper, concrete results are illustrated that highlights the contribution of polarization images in improving the segmentation map that could be extracted from an imaged scene.

2. POLARIZATION IMAGERY

Polarization is a fundamental property of light with as much significance as intensity and color. It provides complementary information about the scene that is largely uncorrelated with other imaging modalities [1]. Any polarization state can be characterized by four real intensity parameters called the Stokes parameters usually expressed as four dimensional column vector called the Stokes vector, $S = [s_0, s_1, s_2, s_3]^T$. Each element of the Stokes vector has a physical interpretation ; s_0 represents lights' total intensity, s_1 and s_2 describe the excess of light in the horizontal and $+45°$ directions respectively, and s_3 is directly connected to the difference between left and right handed circular polarization components in incoming light.

In active optical polarimetry, the scene is illuminated with an incident polarized light controlled by a polarization state generator (PSG). This incident light can be expressed in terms of a Stokes vector S_{in}. The light backscattered from the scene is analyzed by a polarization state analyzer (PSA) composed of a rotating retardation wave plate cascaded with a linear polarizer. Emerging light is then collected by an observation system to form an image on the CCD camera, Fig. 1. The transformation from an incident polarization state S_{in} into an exiting polarization state S_e that occurs to each pixel in the scene represents the polarimetric signature of the imaged scene. Such transformation is commonly described, for each pixel, using a 4×4 linear operator $\mathbf{M}$ known as the Mueller matrix, with $S_e = \mathbf{M}\, S_{in}$.

Let $\mathbf{G}(\theta)_{4\times l}$ be the complete matrix that describes the Stokes parameters of the PSG with l different position θ of its retardation wave plate and let $\mathbf{A}(\theta')_{k\times 4}$ be the complete matrix describing the PSA Stokes parameters with k differ-

ent positions θ' of its retardation plate [2]. The theoretical intensity collected by the observation system is given by:

$$\mathbf{I}\left(\theta,\theta'\right)_{k\times l} \propto \mathbf{A}(\theta')_{k\times 4}\,\mathbf{M}_{4\times 4}\,\mathbf{G}(\theta)_{4\times l}. \qquad (1)$$

The retrieval process of the Mueller matrix **M** is done by inverting relation (1). We define the Mueller image as two-dimensional measurements of the Mueller matrix attached to each pixel of the scene. Such image can reveal contrasts between two different zones having same intensity reflectivity, Fig. 2.

3. POSING OF THE PROBLEM

Because of the mathematical nature of the Mueller matrix, it is impossible to measure its elements directly. Instead, these elements can be retrieved from at least 4×4 polarization intensity measurements through different polarization generated and analyzed states. From these intensity measurements a system of linear equations can be constructed and hence the 16 channels of the Mueller image can be inferred pixel-by-pixel in a least-square sense by inverting relation (1).

In practice, polarization optics forming the polarimeter are never ideal. Therefore performance of the measurement system will degrade. This degradation is represented by a noise term that will be either additive or multiplicative depending upon the illumination light source. Unfortunately due to the presence of a matrix inversion when extracting the Mueller image from relation (1), noise level within the 16 channels of the Mueller image will be amplified. In fact, noise within the 16 channels is estimated to be about two to four times higher than ground truth noise. This value depends on the number of acquisitions, on the choice of wave plates angles selected during the experiment and on the considered channels between the 16 channels.

Further, noise model within the Mueller image does not reflect the real noise model that is infecting the polarimeter. Nevertheless, noise propagation in the first channel m_{00} of the Mueller image always takes the same shape as the real added noise but with a considerable amplification. On the other hand, in the remaining elements of the Mueller image noise takes always a Gaussian distribution regardless of the model of the additive noise that contaminates intensity measurements. Furthermore, noise inside the m_{33} image has the

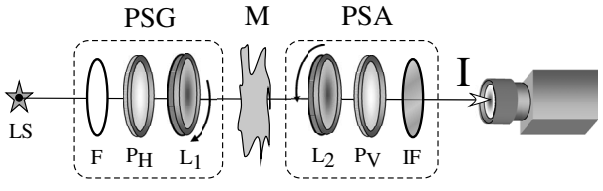

Fig. 1. Classical dual rotating wave plates polarimeter. LS, incoherent light source; F, filter; $P_{H,V}$, horizontal and vertical linear polarizers; $L_{1,2}$, rotating retardation plates; IF, interferential filter.

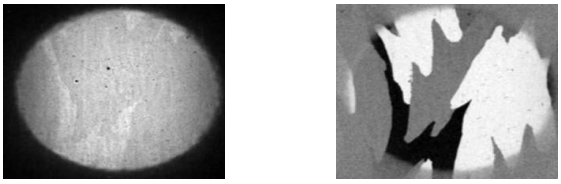

(a) Intensity image (b) Polarization image

Fig. 2. Image of a transparent sheet composed of different polarization properties. (a) Intensity image as seen by a conventional imaging camera. (b) Polarization image acquired by a dual rotating wave plate polarimeter.

lowest value compared to all other 15 channels within the Mueller image, but noise inside this image remains higher than noise infecting raw intensity measurements.

Several papers have covered the segmentation issue performed directly on the Mueller image without considering the physical aspect of noise limitations present inside the Mueller image [3]. In other terms, segmentation was performed on images containing high noise levels instead of directly segmenting raw intensity images with lower noise values. As mentioned in the abstract, this paper will describe a strategy to correctly segment and estimate different classes that are present in a given scene. The segmentation map is extracted from intensity data because noise impact is lower than noise present in the Mueller image. The candidate intensity image(s) that will be selected to segmentation must have a maximum contrast value between all other intensity images. Once a segmentation map is obtained, we will apply it to all the 16 channels of the Mueller image. To that end, we will illustrate by a simulation example that this strategy can attain high levels of accuracy compared to methods based on directly segmenting a specific channel from the Mueller image.

4. NOISE MODEL ESTIMATION

At this stage, a intensity image must be selected for noise model estimation and also for performing segmentation. This intensity image will be chosen based on a contrast criterion. In fact, the selected image is the intensity image having the maximum contrast Γ defined by:

$$\Gamma = \frac{I_{max} - I_{min}}{I_{max} + I_{min}}. \qquad (2)$$

It is believed that this contrast distance reflects the inter-class separability criterion.

Noise model estimation can be described by three main steps: Firstly, apply a Laplacian filter for image suppression. From the resultant image initially estimate the average noise value $\overline{\sigma}_n$. Secondly, suppress the contours by a Canny edge detector. Canny uses thresholds with hysteresis. The higher threshold value of the canny filter is set to be $T_2 = 0.5\overline{\sigma}_n^2 + 2\overline{\sigma}_n + 0.1$, the lower threshold T_1 is 0.4 times the higher

threshold value [4]. Finally, once noise has been isolated from the image, a Kolmogorov-Smirnov test is performed with different probability density functions (pdf) adequation: namely, Gaussian, Gamma and Beta I or II. To this end, propagation noise model infecting the polarimeter is thus estimated by analyzing the most adequate distribution. The estimated noise model will be injected to a dedicated segmentation algorithm, Fig. 3. Here, an Expectation Maximization/Maximum Posterior Mode (EM/MPM) algorithm will be adapted to correctly estimate and segment the noisy image [5]. The MPM algorithm will be regularized by a Hidden Markov Chain model that brings up neighboring information. The parameters are estimated with an EM algorithm [6].

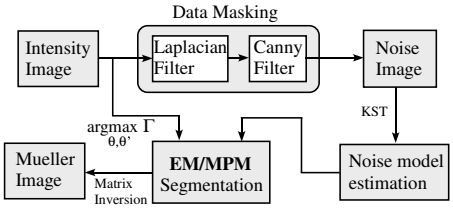

Fig. 3. Noise model estimation algorithm followed by a Maximum Posterior Mode segmentation. The Kolmogorov–Smirnov test is used to measure the reliability of the estimated model.

5. ESTIMATION-SEGMENTATION ALGORITHM

Image segmentation using a HMC model needs to manipulate a vector rather than a 2D image. This can be done thanks to the Hilbert-Peano fractal curve. The major benefit of HMC model for image segmentation resides in its lower computing cost compared to Markov fields. Contrary to hidden Markov fields, the neighboring information is partially conserved in the chain: two neighbors in the chain are neighbors in the image but the reverse is not true. Nevertheless, Hilbert-Peano scan conserves as well as possible neighboring information.

Let us now consider two sequences, a random variable $X = (X_n)_{n\in S}$ the hidden process and $Y = (Y_n)_{n\in S}$ the observed one, with S the finite set of corresponding pixels of an image. Each X_n takes its values in a finite set of K classes $\Omega = \{\omega_1, \omega_2, \cdots, \omega_K\}$. Each Y_n takes its value in the set of real numbers $\mathcal{R}^d$, where d is the number of channels considered. X is a Markov chain of the first order if the influence of a pixel conditionally to its past is reduced to the influence of its predecessor. X can be determined by two parameters: the initial distribution $\pi_i = P(X_1 = \omega_i)$, and the transition matrix $a_{ij}^n = P(X_{n+1} = \omega_j | X_n = \omega_i)$. The chain will be supposed homogeneous, meaning that the transition matrix a_{ij}^n between different classes is independent of the position n within the chain. The segmentation problem is thus to estimate the unobserved hidden labels from the observed realizations.

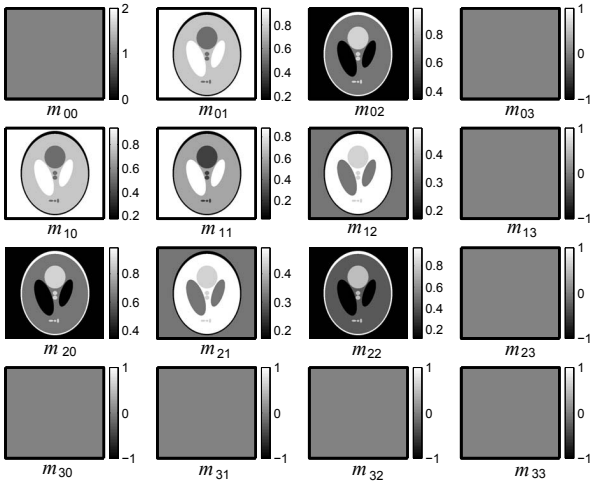

Fig. 4. Mueller image of a modified Shepp–Logan phantom composed of four transparent dichroic substrates. m_{00} corresponds to the intensity image observed by a conventional imaging system.

The *a priori* parameters are clustered in $\Phi_x = \{\pi_k, a_{kl}\}$, and the *data driven* are gathered in $\Phi_y = \{\mu_k, \sigma_k\}$. The aim consists in finding hidden labels X given the observations Y. X can be recovered from the observed process using a Marginal Posterior Mode (MPM) with Baum and Welch forward-backward algorithm [7]. The goal of the MPM algorithm is to minimize the expected value of the number of misclassified pixels. We have based our work on the modified Baums' algorithm that proposes to use conditional probabilities instead of joint probabilities [8]. The forward and backward probabilities can be recursively computed. Forward probabilities $\alpha_n(k)$ are obtained with a recursive computation scanning of the chain from $n = 1$ to $n = N$. Backward probabilities $\beta_n(k)$ are obtained by an inverse scan of the chain. Thus *a posteriori* marginal can be directly computed:

$$P(X_n = \omega_k | Y = y) = \alpha_n(k)\beta_n(k), \quad \forall n \in [1, ..., N] \quad (3)$$

The segmentation of the chain using the MPM criterion requires the maximization of these marginals:

$$\hat{x}_n = \arg_{\omega_k} \max \alpha_n(k)\beta_n(k) \quad (4)$$

6. RESULTS

We have validated this approach on a simulated Shepp–Logan phantom for a single reason that an accurate information about ground truth data can be easily obtained, Fig 4. Thus an error analysis of the segmentation algorithm can be correctly carried out. This phantom is made up of four different classes, each has a different polarimetric property. Physically it can be fabricated from transparent layers, with each class having a modified dichroism, which make it impossible to any segmentation algorithm reposing on a conventional imaging system

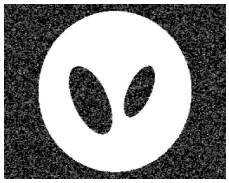

(a) m_{02}

(b) Intensity

Fig. 5. EM/MPM segmentation performed on the m_{02} image and on the maximum contrasted intensity image.

to extract any feature from this phantom. The added noise is Gaussian with an estimated signal-to-noise ratio (SNR) ≈ 10 dB.

As illustrated in figure 5, the EM/MPM algorithm could not correctly segmented the noisy m_{02} channel of the Mueller image despite that this channel has the best inter-class separability compared to all other channels. In contrast, the same algorithm has correctly segment the corresponding intensity image having the highest contrast.

In fact, due to the presence of a matrix inversion when retrieving the Mueller image a noise amplification has occurred. This amplification has reduced the classes separability. Thus the EM step that is mainly initiated by a K–means algorithm has wrongly estimated each class mean and variance for the m_{02} channel. In contrast, when the same algorithm was performed on the intensity image the four different classes were sufficiently separated to allow to the K-means coupled to the EM algorithm to correctly estimate each class's mean and variance. The MPM step is performed more smoothly and the HMC neighboring will favor the homogeneity within each class. The obtained segmentation map will be applied to all the 16 channels of the Mueller image. The Mueller matrix for each class can be thus estimated. To that end, the Frobenius error between each estimated class with its expected theoretical matrix will be also calculated.

In figure 6 (a) we have plotted the histogram of the Frobenius norm error percentage between the simulated Mueller image and the noisy one. Noise impact on the Mueller image is remarkably disturbing (average error ≈ 80 %). In contrast, the EM/MPM algorithm when applied to the maximum contrasted intensity image has revealed these four classes. When comparing the theoretical matrix of each class with the estimated one, error propagation was limited to less than 1.4% inside each estimated class of the Mueller image, Fig 6 (b).

7. CONCLUSION

We have illustrated in this work a strategy that improves segmentation maps using polarization images instead of conventional ones. An accurate segmentation map can thus be obtained based on the physical properties of different objects present in the scene rather than their intensity reflectivity. Segmentation map is extracted from the polarimetric intensity image having the maximum contrast. Simulation results have shown the robustness of this method compared to methods based on segmenting a specific channel from the Mueller image. For extremely high noise levels, a multimodale technique must be used ; as expected results of a multimodale HMC segmentation performed on raw intensity data outperforms the multimodale HMC segmentation results inferred from the 16 channels of the Mueller image.

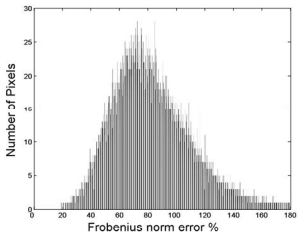

(a) Matrix Inversion

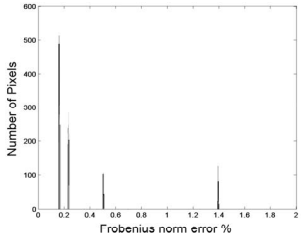

(b) EM/MPM

Fig. 6. Frobenius norm error distribution for the noisy Shepp–Logan phantom. (a) result after inversion. (b) result after the EM/MPM estimation-segmentation algorithm performed on the maximum contrasted polarization intensity image.

8. REFERENCES

[1] J. S. Tyo, D. L. Goldstein, D. B. Chenault and J. A. Shaw, " Review of passive imaging polarimetry for remote sensing applications," Appl. Opt. **45:** 5453-5469, 2006.

[2] R. A. Chipman, *Handbook of Optics*, vol. II, 2nd Ed. M. Bass ed. (McGraw-Hill, 1995).

[3] C. Collet, J. Zallat and Y. Takakura, " Clustering of Mueller matrix images for skeletonized structure detection," Opt. Express **12:** 1271-1280, 2004.

[4] C. Liu, W. T. Freedman, R. Szeliski and S. B. Kang, " Noise estimation from a single image," *IEEE* CVPR'06, 2006.

[5] M. L. Comer and E. J. Delp, " The EMMPM algorithm for segmentation of textured images: analysis and further experimental results, " *IEEE* Transactions on Image Processing, **9:** 1731-1744, 2000.

[6] A. Dempster, N. Laird and D. Rubin, " Maximum Likelihood for incomplete data via the EM algorithm," J. Royal Statistical Society, B. **39:** 1-38, 1977.

[7] L. E. Baum, T. Petrie, G. Soules, and N. Weiss, " A maximization technique occurring in the statistical analysis of probabilistic functions of Markov chains," Ann. Math. Statist. **41:** 164-171, 1970.

[8] P. A. Devijver, " Baum's Forward–Backward algorithm revisited," Pat. Recogn. Lett. **3:** 369-373, 1985.